ResearchGate

See discussions, stats, and author profiles for this publication at: http://www.researchgate.net/publication/230959430

Closed-form studies of a new hybrid damping technique using an active layer and hard-coated damping alloys

ARTICLE *in* SMART MATERIALS AND STRUCTURES · MARCH 2007

Impact Factor: 2.5 · DOI: 10.1088/0964-1726/16/3/009

READS

9

3 AUTHORS, INCLUDING:

Bishakh Bhattacharya

Indian Institute of Technology Kanpur

62 PUBLICATIONS **150** CITATIONS

SEE PROFILE

Available from: Bishakh Bhattacharya

Retrieved on: 29 September 2015

Smart Mater. Struct. **16** (2007) 626–633 doi:10.1088/0964-1726/16/3/009

Closed-form studies of a new hybrid damping technique using an active layer and hard-coated damping alloys

S Ahlawat[1], B R Vidyashankar[2] and B Bhattacharya[1,3]

[1] Department of Mechanical Engineering, IIT-Kanpur, Kanpur 208016, India
[2] GM India Technical Centre, 3rd floor, Creative Building, Bangalore 560066, India

E-mail: bishakh@iitk.ac.in

Received 15 February 2006, in final form 6 February 2007
Published 30 March 2007
Online at stacks.iop.org/SMS/16/626

Abstract
Hybrid damping of structural vibration using a combination of active and passive layers is found to have high application potential due to the requirement of a lower power supply and guaranteed stability. Use of hard-coating layers as a passive damping treatment is found to be industrially acceptable for turbine blades etc, due to the high damping capacity and large service temperature range. However, such damping materials also have high strain dependence. In a way that is similar to active constrained layer damping, by using an active material the strain in the passive damping can be controlled, and thereby the damping performance of the passive layer. This paper proposes a semi-analytical method to estimate structural damping in such a system and obtain the response of a smart hybridly damped system. The paper delves into the closed-form solution of all common boundary conditions of a vibrating beam, namely cantilever, hinged–hinged, free–free, hinged–free, and fixed–fixed beams. It also compares the damping performance of a beam with only a passive damping layer to that of beams comprising both active and passive damping layers.

(Some figures in this article are in colour only in the electronic version)

List of symbols

η	mean loss factor
ρ	density of the plate
ω	modal frequency of the beam
ε_a	active strain in the host beam
E	modulus of elasticity
E_i	total energy in the system at the ith instant
I	moment of inertia
$\bar{C}$	modal constant for beam vibration
M	modal loss factor of the beam
t_v	thickness of the hard-coated damping layer,
t_c	thickness of the top structural layer
t_a	thickness of the bottom structural layer
m	total mass of the beam
n	number of time-segments in one oscillation
m_s	number of segments of the active beam
I_p	current applied on the smart magnetostrictive actuator

[3] Author to whom any correspondence should be addressed.

Introduction

Smart materials like piezoceramics, magnetostrictive materials and shape memory alloys have been investigated for active vibration control application over the last decade. Major concerns related to the use of such materials have been the availability of limited dynamic strain, on-board power supply and robustness [1]. Active constrained layer damping (ACLD) of structures using piezoelectric actuators as smart materials has emerged as a trade-off solution [2, 3] between active and passive damping, and has shown significant application potential due to higher energy dissipation to weight characteristics. The success of this technique has been shown to be influenced by the capacity of shear deformation of the active constraining layer made of piezoceramic or magnetostrictive material [4, 14].

Tani *et al* [5] have reviewed extensively the uses of active materials for vibration control and have shown that smart magnetostrictive actuators based on Terfenol-D material can generate comparatively larger strokes for the same power and have good potential for active damping. With the advent of particulate magnetostrictive composites [6, 7], it is found that such a material could also be used in a layered form over a host beam to introduce distributed control of vibration. However, in general, magnetostrictive composites do not possess good inherent structural damping. Hence, in highly flexible structures like helicopter rotor blades and remote arm manipulators, active control using such materials may lead to instability due to poor observability/controllability of the system. It is expected that a thin layer of passive damping coating could enhance the stability of the system in such circumstances without any significant weight penalty.

Lim *et al* [8] have proposed a new strategy of ACLD-based damping in which a viscoelastic material is sandwiched between the host structure (made of aluminium) and active piezo-layer. An attractive three-dimensional (3D) finite-element model has been developed by representing the frequency-dependent damping of the viscoelastic material as a series of second-order oscillators in the Laplacian domain. This has facilitated a time-domain solution of the ACLD-based vibrating system. Bhattacharya *et al* [9] have applied the finite-element method (FEM) in numerical modelling of different types of smart ACLDs, and they have studied the performance of combined damping in composites, using both active and passive damping layers. It was observed by Karimmi *et al* [10] that hard coatings of Fe–Cr alloy could be used effectively for passive damping. Unlike the situation with viscoelastic materials, the passive damping in such cases is dependent on the applied strain, and it requires a different approach to model the dynamic behaviour. Bhattacharya *et al* [11] have proposed a new type of ACLD for vibration control of systems having an active layer and strain-dependent damping layer as the coating over host beams. Their formulation expressed the generalized displacement matrix in terms of nodal displacements using the FEM approach and used this to compute the strains. They explored the active only, passive only and hybrid damping cases separately. The effect of active damping was incorporated by applying the extended Hamilton's principle and recomputing the strain from the undamped displacement vector. New damping (C) and stiffness (K) matrices were computed and used in the equation of motion (due to the strain dependence of the loss factor in the passive layer) to obtain the frequency response function (FRF). The numerical scheme was iterated several times until convergence in the frequency response was achieved. Thus, the scheme was not advantageous from the computational point of view and difficult to implement in real-time control.

In this paper, a closed-form hybrid control scheme related to the vibration of beams for different boundary conditions is proposed. A multilayer beam comprising host layers, a strain-dependent passive damping layer and an active layer

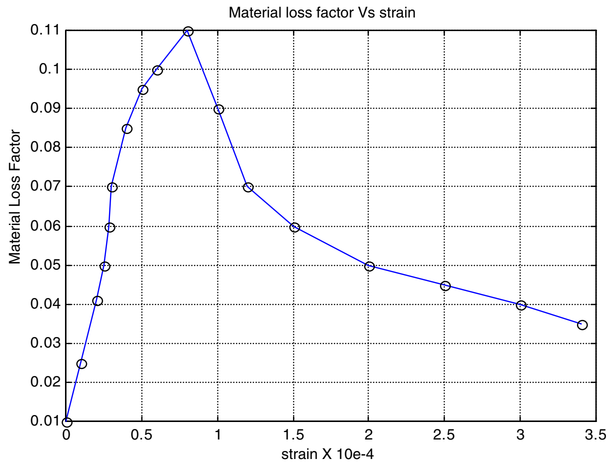

Figure 1. Variation of material loss factor versus strain amplitude for a typical hard-coated damping material of Fe–Cr alloy as reported by Karimmi *et al* [10] used as a passive damping layer.

is considered. The passive damping layer is arranged either sandwiched or in an Oberst beam configuration. Usually, for a specific range of strain, the loss factor in the damping material may be an order of magnitude higher that the average damping, while for some other range of strain it may become extremely low. A typical strain-dependent damping is depicted in figure 1. Damping applications of similar coatings have recently been reported by Patsias *et al* [12]. The introduction of an active layer gives a means by which the strain in the hard-coated damping layer can be controlled directly or indirectly so as to derive maximum or optimal damping from the passive layer. This external control is obtained by applying an external voltage field in the case of piezo-composites or external current in the case of magnetostrictive composites. Typically the feedback-based control works on the following principle.

The vibrations induce a strain in the passive damping material (referred to also as a 'hard-coat' layer), which in conjunction with the induced active strain governs the resultant loss factor of the damping layer. However, due to the dynamic nature and strain dependence, the loss factor in the material is also a function of time. Hence, in a closed-loop system, the active strain required to maximize the loss factor of the passive layer is to be determined at each time instant. The active strain is appropriately changed through the voltage/current applied. Hence, closed-form estimation of the temporal dependence of the external current would enable real-time vibration control in such cases.

Section 1 introduces the closed-form modelling of free vibration in a multilayered beam corresponding to different boundary conditions. Section 2 has developed the closed-form analysis corresponding to passive damping using the modal strain energy method. In section 3, the method is further extended to include active damping assuming a simple velocity-proportional feedback control. Finally, in section 4 different case studies are provided corresponding to various arrangements of the active and passive damping layers.

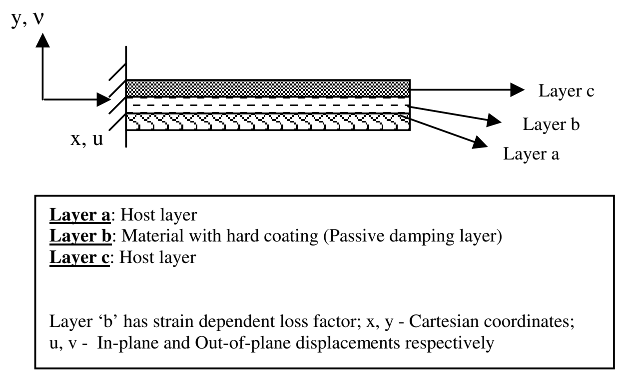

Figure 2. General configuration of a three-layered beam.

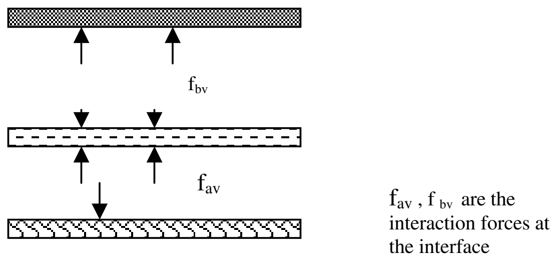

Figure 3. Free-body diagram of a multilayer beam.

1. Modelling of free vibration in a multilayered beam with different boundary conditions

1.1. Undamped model of a hybrid beam

In order to establish the significance of some new terms that will be used to quantify the damping of vibration, a succinct study of undamped cantilever vibration is presented here. The cantilever multilayered beam model is shown in figure 2.

The transverse equation of motion for the different layers of the beam (as shown in figure 2) may be expressed as

$$-\frac{\partial^2}{\partial x^2}\left(E_{\mathrm{a}}I_{\mathrm{a}}\frac{\partial^2 v}{\partial x^2}\right) + f_{av} = m_{\mathrm{a}}t_{\mathrm{a}}\frac{\partial^2 v}{\partial t^2} \tag{1a}$$

$$-\frac{\partial^2}{\partial x^2}\left(E_{\mathrm{b}}I_{\mathrm{b}}\frac{\partial^2 v}{\partial x^2}\right) - f_{av} + f_{bv} = m_{\mathrm{b}}t_{\mathrm{b}}\frac{\partial^2 v}{\partial t^2} \tag{1b}$$

$$-\frac{\partial^2}{\partial x^2}\left(E_{\mathrm{c}}I_{\mathrm{c}}\frac{\partial^2 v}{\partial x^2}\right) - f_{bv} = m_{\mathrm{c}}t_{\mathrm{c}}\frac{\partial^2 v}{\partial t^2} \tag{1c}$$

where v is the displacement relative to the natural undisturbed configuration of the beam; f_{av} denotes the interaction force between the two layers in the 'y' direction (as shown in figure 3). The interaction in the form of shearing force between the layers is neglected in this model since the thickness of the host beam is very large in comparison to the coating layers b and c.

Considering the entire beam, the transverse equation of motion may be written as

$$-\frac{\partial^2}{\partial x^2}\left((E_{\mathrm{a}}I_{\mathrm{a}} + E_{\mathrm{b}}I_{\mathrm{b}} + E_{\mathrm{c}}I_{\mathrm{c}})\frac{\partial^2 v}{\partial x^2}\right) = (m_{\mathrm{a}}t_{\mathrm{a}} + m_{\mathrm{b}}t_{\mathrm{b}} + m_{\mathrm{c}}t_{\mathrm{c}})\frac{\partial^2 v}{\partial t^2}. \tag{2}$$

Alternatively,

$$-\frac{\partial^2}{\partial x^2}\left(EI\frac{\partial^2 v}{\partial x^2}\right) = mt\frac{\partial^2 v}{\partial t^2} \tag{3}$$

where

$$EI = E_{\mathrm{a}}I_{\mathrm{a}} + E_{\mathrm{b}}I_{\mathrm{b}} + E_{\mathrm{c}}I_{\mathrm{c}}$$

$$mt = m_{\mathrm{a}}t_{\mathrm{a}} + m_{\mathrm{b}}t_{\mathrm{b}} + m_{\mathrm{c}}t_{\mathrm{c}}.$$

Applying the appropriate boundary conditions and variable separation, the standard solution for the response may be written as

$$Y = c_1\sin(\beta x) + c_2\cos(\beta x) + c_3\sinh(\beta x) + c_4\cosh(\beta x). \tag{4}$$

Using the boundary conditions, β is evaluated and three of the constants may be evaluated in terms of the constant c_1. The term c_1 is then taken out and serves the purpose of quantifying the amplitude of vibrations. This term is designated as $\bar{C}$, and it is assigned a value of unity initially. As the vibrations of the beam die down due to damping, $\bar{C}$ reduces to zero. Dividing each period of oscillation into sufficiently small intervals, and applying the undamped response over each time interval, $\bar{C}$ for any instant of vibration may be found by taking into account the effect of energy dissipation in the previous instant.

Thus the complete solution of the differential equation for undamped cantilever vibration may be written as

$$v = \bar{C}(\sin(\beta x) + c_2'\cos(\beta x) + c_3'\sinh(\beta x) + c_4'\cosh(\beta x))\sin(\omega_n t). \tag{5}$$

The values of the modal constants and β may be obtained from any standard text [15].

2. Analysis of passively damped beams using the modal strain energy (MSE) method

In this section the procedure to model passively damped vibration using the equations for undamped oscillation is formulated. The time interval of an oscillation may be divided into suitable small time segments, and the undamped response may be coupled with the $\bar{C}$ multiplier that embodies the effect of energy dissipation. Reduction of the value of the $\bar{C}$ multiplier in every successive time step in consonance with the energy dissipated in earlier time segments incorporates the damping effect.

The length of the beam may be divided into suitably small length segments (figure 4) and the strain induced in each segment at a particular time instant is computed. A temporal discretization scheme that uses the value of $\bar{C}$ at a particular time instant for computing $\bar{C}$ at the next time instant is proposed. Let m denote the number of length divisions in the beam and n denote the number of segments into which one oscillation time period is divided. Denoting each time segment by Δt, and the kth modal frequency by ω_k,

$$\Delta t = \frac{2\pi}{n\omega_k}.$$

First, the strain in the beam is computed for the required time instant using the Euler–Bernoulli beam model. Next,

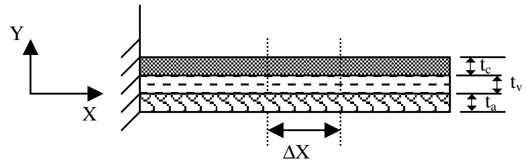

Figure 4. Multilayer beam with the passive damping material in the middle.

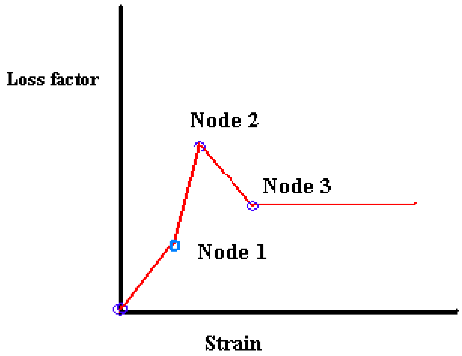

Figure 5. A three-parameter variation of loss factor versus strain for a hard-coated material layer.

depending on the location of the passive (hard-coated) damping layer, the strain experienced in the hard-coated damping layer is computed for that time instant. It may be noted that the hard-coated damping layer could either be sandwiched between two layers or it could be applied as a free-standing layer on the top or the bottom of the beam. First, the damping layer is considered to be fixed between two host layers. At a particular location along the length of the beam, strains may be computed and the mean value of strain across the beam's cross section may be computed. This process is elucidated as follows.

Let t_{v} denote the thickness of the damping layer, t_{c} the thickness of the upper host layer and t_{a} the thickness of the bottom host layer.

$$\varepsilon_x = \frac{\int_{t_1}^{t_2} \varepsilon(x, y)\partial y}{t_{\mathrm{v}}} = \left|\frac{t_{\mathrm{c}} - t_{\mathrm{a}}}{2}\right| \frac{\partial^2 v}{\partial x^2} \tag{6}$$

$$t_2 = t_{\mathrm{c}} + t_{\mathrm{v}} - \frac{t_{\mathrm{a}} + t_{\mathrm{v}} + t_{\mathrm{c}}}{2}; \qquad t_1 = \left(-\frac{t_{\mathrm{a}} + t_{\mathrm{v}} + t_{\mathrm{c}}}{2} + t_{\mathrm{c}}\right).$$

If the damping layer is assumed to be at the top or the bottom of the beam,

$$\varepsilon_x = \frac{\int_{t_1}^{t_2} \varepsilon(x, y)\partial y}{t_{\mathrm{v}}} = \left(\frac{t_{\mathrm{c}} + t_{\mathrm{a}}}{2}\right) \frac{\partial^2 v}{\partial x^2} \tag{7}$$

$$t_2 = \frac{t_{\mathrm{a}} + t_{\mathrm{v}} + t_{\mathrm{c}}}{2}; \qquad t_1 = \left(t_{\mathrm{a}} + t_{\mathrm{c}} - \frac{t_{\mathrm{a}} + t_{\mathrm{v}} + t_{\mathrm{c}}}{2}\right).$$

Subsequently, the loss factor in the damping layer is determined from the parametric curve of loss factor versus strain (see figure 5). The variation of loss factor versus strain for an actual material is approximated from figure 1 by line segments using three points between which the variation is assumed to be linear. Based on material specification, the three nodes can be specified to simulate the actual variation of loss factor with strain based on the material specification [10].

The mean loss factor may be computed for the current instant along the length of the hard-coated damping layer by taking the arithmetical mean of the loss factors of m_{s} segments.

$$\eta(t) = \frac{\sum_{j=1}^{m} \eta_j(t)}{m_s} \tag{8}$$

where η denotes the mean loss factor.

The next step is to obtain the amplitude $\bar{C}_{i+1}$ in terms of $\bar{C}_i$, where the index 'i' denotes the ith time instant of an oscillation. The loss factor for any temporal segment may be expressed as

$$\eta_i = \frac{n W_{\mathrm{dissipated}}}{2E_i\pi} \tag{9}$$

where E_i denotes the total energy of the beam at the beginning of the ith instant.

$$W_{\mathrm{dissipated}} = \frac{2E_i\eta_i\pi}{n}. \tag{10}$$

Also since:

$$E_{i+1} = E_i - W_{\mathrm{dissipated}}. \tag{11}$$

The energy term E_i includes both the kinetic and the potential energy of the beam. The kinetic energy and the potential energy are computed in terms of $\bar{C}_i$. Accordingly,

$$\begin{aligned} T_i &= \int\int\int \tfrac{1}{2}(\dot{y})^2 \,\mathrm{d}m = \tfrac{1}{2}\omega^2 \int\int\int y^2 \,\mathrm{d}m \\ &= \frac{b\omega^2}{2}(\rho_{\mathrm{a}}t_{\mathrm{a}} + \rho_{\mathrm{v}}t_{\mathrm{v}} + \rho_{\mathrm{c}}t_{\mathrm{c}})\cos^2(\omega_k t)(\bar{C}_i)^2 \\ &\quad\times \int_0^L (\sin(x\beta) + c_2'\cos(x\beta) + c_3'\sinh(x\beta) \\ &\quad + c_4'\cosh(x\beta))^2 \,\mathrm{d}x \qquad \text{at } t = \frac{2\mathrm{i}\pi}{\omega_k n}. \end{aligned} \tag{12}$$

The expression for T_{i+1} may be obtained similarly by substituting the index $i+1$ by I at $t = \frac{2(i+1)\pi}{\omega_k n}$.

Next, the potential energy, V_i, is calculated as follows.

$$\begin{aligned} V_i &= \tfrac{1}{2}\bar{C}_i^2(E_{\mathrm{a}}I_{\mathrm{a}} + E_{\mathrm{v}}I_{\mathrm{v}} + E_{\mathrm{c}}I_{\mathrm{c}})(\beta_k)^4 \sin^2(\omega_k t) \\ &\quad\times \int_0^L (-\sin(x\beta_k) - c_2'\cos(x\beta_k) + c_3'\sinh(x\beta_k) \\ &\quad + c_4'\cosh(x\beta_k))^2 \,\mathrm{d}x \qquad \text{at } t = \frac{2\mathrm{i}\pi}{\omega_k n}. \end{aligned} \tag{13}$$

As with the kinetic energy, the expression for V_{i+1} may be obtained after substituting the index i by $i+1$.

An additional term appears in the expression of potential energy that may be considered to be due to stretching. The additional term is given by

$$\begin{aligned} &\frac{1}{2}\int_0^L \frac{E_{\mathrm{a}}I_{\mathrm{a}} + E_{\mathrm{v}}I_{\mathrm{v}} + E_{\mathrm{c}}I_{\mathrm{c}}}{4}\left(\frac{\mathrm{d}y}{\mathrm{d}x}\right)^4 \mathrm{d}x \\ &= \frac{E_{\mathrm{a}}I_{\mathrm{a}} + E_{\mathrm{v}}I_{\mathrm{v}} + E_{\mathrm{c}}I_{\mathrm{c}}}{8}(\beta_k)^4\bar{C}_i^2\sin^4(\omega_k t)\int_0^L (\cos(x\beta_k) \\ &\quad - c_2'\sin(x\beta_k) + c_3'\cosh(x\beta_k) + c_4'\sinh(x\beta_k))^4 \,\mathrm{d}x \\ &\quad \text{at } t = \frac{2\mathrm{i}\pi}{\omega_k n}. \end{aligned} \tag{14}$$

Following energy conservation,

$$V_{i+1} + T_{i+1} = V_i + T_i - \Delta E$$

where

$$\Delta E = \frac{2\pi(\eta_a(V_{i_a} + T_{i_a}) + \eta_h(V_{i_c} + T_{i_c}) + \eta_v(V_{i_v} + T_{i_v}))}{n}. \tag{15}$$

η_v is calculated from the plot of strain versus loss factor.

Using equations (12)–(15), we calculate $\overline{C_{i+1}}$ in terms of $\bar{C}_i$ and progress in time, recomputing the value of the modal constant after every time segment.

2.1. *Calculation of the modal loss factor*

The modal loss factor for the vibrating beam may be defined as

$$\text{Modal loss factor (at } i\text{th time instant)} = \frac{\sum_{j=1}^{m} V_{i_j}\eta_j}{\sum_{j=1}^{m} V_{i_j}}. \tag{16}$$

The potential energy terms have been formulated for different length segments. These are used to obtain the modal loss factor as a function of time (since the loss factor of the hard-coated damping layer varies with time).

For the case when the beam boundary conditions are not those of fixed–fixed type, the equation for modal loss simplifies to

$$M = \frac{\sum_{j=1}^{m} E_a I_a \eta_a(j) + \sum_{j=1}^{m} E_c I_c \eta_h(j) + \sum_{j=1}^{m} E_v I_v \eta_v(j)}{E_a I_a + E_v I_v + E_c I_c}. \tag{17}$$

This is because the integrals common to both numerator and denominator cancel out. For the case of a fixed–fixed beam, because of the existence of the two terms in the potential energy, the expression becomes

$$M = \left\{\left(\sum_{j=1}^{m} \tfrac{1}{2} E_a I_a \eta_a(j) + \sum_{j=1}^{m} \tfrac{1}{2} E_c I_c \eta_h(j) + \sum_{j=1}^{m} \tfrac{1}{2} E_v I_v \eta_v(j)\right) \sin^2(\omega_k t)\, I_1 + \left(\sum_{j=1}^{m} \tfrac{1}{8} E_a I_a \eta_a(j) + \sum_{j=1}^{m} \tfrac{1}{8} E_c I_c \eta_h(j) + \sum_{j=1}^{m} \tfrac{1}{8} E_v I_v \eta_v(j)\right) \sin^4(\omega_k t)\, I_2\right\} \left\{\sum V_i\right\}^{-1} \tag{18}$$

$$I_2 = \int_0^L (\cos(x\beta_k) - c_2' \sin(x\beta_k) + c_3' \cosh(x\beta_k) + c_4' \sinh(x\beta_k))^4 \, dx$$

$$I_1 = \int_0^L \left(-\sin(x\beta_k) - c_2' \cos(x\beta_k) + c_3' \sinh(x\beta_k) + c_4' \cosh(x\beta_k)\right)^2 \, dx.$$

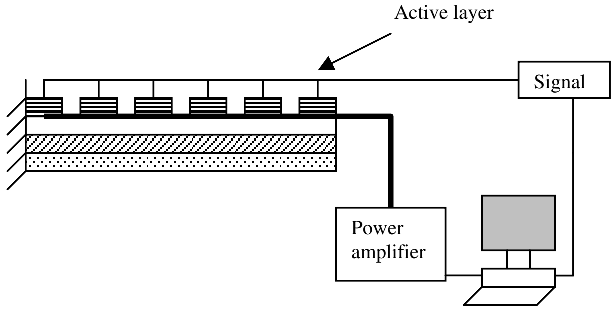

Figure 6. Closed-loop control of beam vibrations with the active layer on the top.

3. A closed-loop system (active layer operative)

An active layer is now introduced (figure 6) and the external current required for rapid damping of beam vibrations is determined. A thin layer of active material is spread over the beam. This active layer is applied on beam segments, and for ease of modelling, it is assumed that the active layer is applied at alternate length segments into which the beam has been divided (number of segments is m in number).

Sufficient strain in the beam is introduced (through the active element) so that the strain of the hard-coated damping layer corresponds to the maximum loss factor. However, since this maximum loss factor condition cannot be met exactly at all the points of the hard-coated damping layer at a particular instant of beam vibration, the method of least squares is employed to get the value of optimum voltage to be applied at a particular instant.

First, the active strain shared by the hard-coated damping layer is determined. Absence of shear force is assumed in the analysis.

The discussion is split into two cases: when the hard-coated damping layer is sandwiched between two host layers and when it is on top of the beam, just below the active layer (of thickness t). The case when the hard-coated damping layer is the bottommost layer is dynamically equivalent to the case when it is on the top.

3.1. *Case I: Hard-coated damping layer sandwiched*

The mean active strain at a particular distance (figure 7) across the thickness of the hard-coated damping layer is

$$\overline{\varepsilon_{x,a}} = \frac{2\varepsilon_a}{t_a + t_c + t_v + t}\left(\frac{\int_{-t_v/2}^{t_v/2}\left(\frac{t_c+t-t_a}{2} + z'\right) dz'}{t_v}\right) = \frac{\frac{t_c+t-t_a}{2}}{\frac{t_a+t_c+t_v+t}{2}}\varepsilon_a = \frac{t_c + t - t_a}{t_a + t_c + t_v + t}\varepsilon_a. \tag{19}$$

3.2. *Case II: Oberst beam with hard-coated damping layer at the top next to the smart actuator*

For this case, the mean active strain experienced by the hard-coated damping layer (figure 8) at a particular distance is computed:

$$\overline{\varepsilon_{x,a}} = \frac{t_c + t + t_a}{t_a + t_c + t_v + t}\varepsilon_a. \tag{20}$$

Table 1. Details of layer-wise material parameters of the smart laminate.

Material	Thickness (m)	Elastic modulus (GPa)	Density (kg m^{-3})	Loss factor, η
Aluminium	0.01	70	2700	0.001
Host layer II	150×10^{-6}	70	2700	0.001
Hard-coated damping layer (Fe–Cr–Al alloy)	150×10^{-6}	200	7000	(loss factor as in figure 1)
Terfenol-D [13] composite	0.001	35	9250	[a]

[a] Magneto-mechanical constant $= d_{31} = 1.67 \times 10^{-8}$ mA^{-1}.

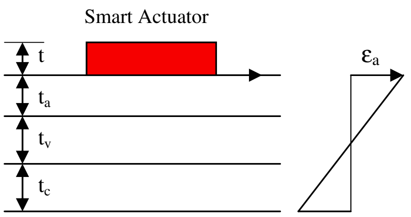

Figure 7. Active strain propagated through the beam's cross section.

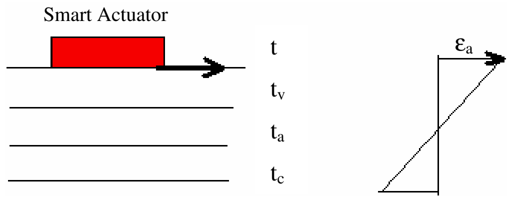

Figure 8. Active strain directly induced in the damping layer (t_v).

From these two cases, it can be written that the strain in the hard-coated damping layer at a particular distance is $k\overline{\varepsilon_{x.a}}$, where k is the appropriate factor, as the case may be. Let $\overline{\varepsilon_{x.p}}$ denote the strain due to passive vibration. Using the method of least squares, we attempt to minimize the following function:

$$f = \sum_{i=1}^{m} \left(\overline{\varepsilon_{x.a}} + \overline{\varepsilon_{x.p}} - \varepsilon_{\max .\mathrm{lossfactor}}\right)_i^2. \tag{21}$$

ε_a is determined from $\overline{\varepsilon_{x.a}}$. We know that $\varepsilon_\mathrm{a} = k\overline{\varepsilon_{x.a}}$. Differentiating, we obtain

$$\frac{\mathrm{d}f}{\mathrm{d}\varepsilon_\mathrm{a}} = 0 = \sum_{i=1}^{m} 2\left(\overline{\varepsilon_{x.a}} + \overline{\varepsilon_{x.p}} - \varepsilon_{\max .\mathrm{lossfactor}}\right)_i k$$

$$\Rightarrow k\varepsilon_\mathrm{a} = \varepsilon_{\max .\mathrm{lossfactor}} - \frac{\sum_{i=1}^{m}\left(\overline{\varepsilon_{x.p}}\right)_i}{m}$$

$$\Rightarrow \varepsilon_\mathrm{a} = \frac{\varepsilon_{\max .\mathrm{lossfactor}} - \frac{\sum_{i=1}^{m}\left(\overline{\varepsilon_{x.p}}\right)_i}{m}}{k}. \tag{22}$$

Finally, the applied external current is obtained as

$$I_p = -K_\mathrm{c}\,\mathrm{sgn}(\varepsilon_\mathrm{a})\frac{t\,|\varepsilon_\mathrm{a}|}{d_{31}} \tag{23}$$

where K_c is the control constant.

Once ε_a is obtained for a time instant, the loss factors for the hard-coated damping layer (in the segments having an active layer) are calculated. The energy dissipated is obtained, and after recalculating $\bar{C}_i$ by the elucidated procedure, the next time step is considered.

4. Results and discussion

For numerical studies, a composite beam fixed at both ends is considered. The beam is initially composed of three layers: two structural layers and one layer of hard-coated damping material (see table 1 for the material properties) that provides the passive damping. An active layer is subsequently introduced over this beam. The host beam material is taken to be isotropic and homogeneous. Two possible ways of arranging the hard-coated damping layer are considered in this study: sandwiched in the middle or placed at the top. The dimensions of the beam layers along with their material constants are specified below:

- length of the beam: 1 m;
- number of oscillations simulated: 1000;
- segments into which the length of the beam has been divided: 10;
- segment into which an oscillation is divided: 10.

The amplitudes of vibration corresponding to the first bending mode are shown in figures 9 and 10 for the sandwiched and Oberst configurations respectively. In both cases the hybrid damping could successfully damp the amplitude. Also, in both cases, the hybrid damping scheme has shown high reduction of amplitude in comparison to the passive damping scheme. With hybrid damping, in the case of the sandwiched configuration the time taken to reach 10% of the initial amplitude was about 26 s, while that for the Oberst case was only 14 s. The efficiency of the active layer was clearly higher when the hard damping layer was placed just adjacent to it.

Certain hard-coated damping layers do not show the typical three-point feature of change in loss factor as assumed in the first case. For such materials, the material damping stabilizes to a particular value beyond a certain specified strain [16]. The closed-form analysis for hybrid and passive only damping is carried out similarly for such cases. The results are presented in figures 11 and 12. It may be noted that here again hybrid damping has shown significantly better results for both sandwiched and Oberst configurations. With hybrid damping, in the case of the sandwiched configuration the time taken to reach 10% of the initial amplitude was about 14 s, while that for the Oberst case was only 3 s. Also, the Oberst configuration has shown better performance in comparison to the sandwiched configuration. A possible reason for the better performance of the Oberst configuration is due to the adjacency of the smart layer to the coating. This has

Table 2. Comparison of loss factors for the smart beam evaluated by the FE technique [11] and closed-form analysis, respectively.

Mode no.	Frequency (FE) (Hz)	Frequency (closed form) (Hz)	Modal damping (FE) (%)	Modal damping (closed form) (%)
I	28.8	28.8	2.1	2
III	150.3	149.4	4.0	4.5
V	375.4	369.9	4.1	4.7

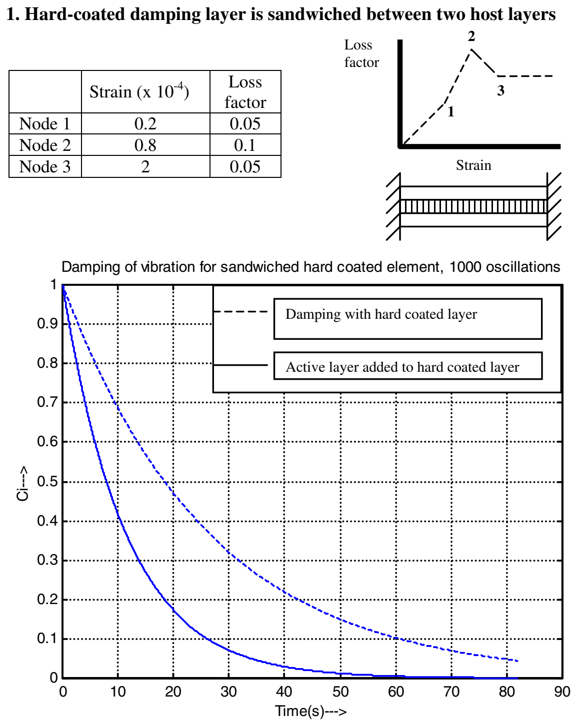

Figure 9. Damping of vibration using a hard-coated damping layer sandwiched between the host layers, and using a combination of an active layer with a hard-coated damping layer.

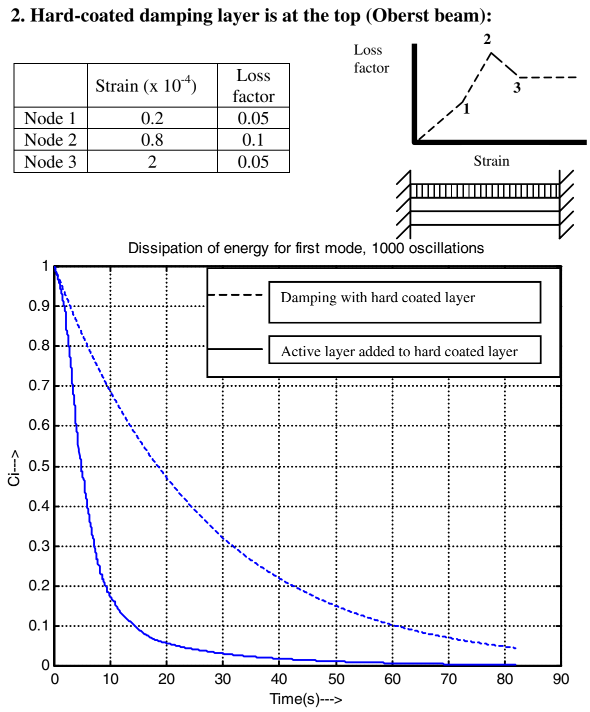

Figure 10. Damping of vibration using a hard-coated Oberst damping layer, and using the same in combination with an active layer.

caused direct control of applied strain up to an optimal level and hence resulted in higher damping.

The loss factors related to the first three odd modes of vibration evaluated by the iterative FE technique [11] and closed-form analysis are given in table 2. The iterative technique is based on a simple four degrees of freedom beam element consisting of in-plane displacement, out-of-plane displacement, slope, and voltage at the piezo-patch. For FE analysis the beam is divided into ten elements and the results are reported after six iterations. The results show that both FEM and closed-form results agree quite well for all three odd modes of vibration of the beam. However, the finite-element analysis has underestimated the modal damping for higher modes, which may be due to the limitation in number of iterations and mesh refinement.

Finally, studies were carried out on the settling time of the amplitude of vibration for the same beam with the sandwiched damping layer corresponding to different modal vibrations. The results obtained for the first three nodes are presented in table 3. The table shows that even for the higher modes of vibration the proposed scheme is quite successful compared with conventional passive damping.

Table 3. Comparison of settling time for different modes of vibration with and without the hybrid control scheme.

Mode number	Settling time (hybrid) (s)	Settling time (passive) (s)
I	26	32
II	7	11
III	2.9	4.6

5. Conclusions

Closed-form analysis of hybrid damped systems based on the modal strain energy method and discrete time computation of the loss factor is proposed. The closed-form results will facilitate parametric studies of this complex system to obtain optimal layer configuration and necessary control gain. The superiority of the hybrid damping scheme over a fully passive damping scheme is established. The damping is found to be more efficient when the hard-coating layer is placed adjacent to the smart patches. The studies also matched quite well with the results of an iterative finite element analysis. The method could be extended in the future to take into account both strain-dependent and frequency-dependent damping materials.

3. Oberst case (hard-coated damping layer is Sandwiched)

	Strain (X10^{-4})	Loss factor
Node 1	0.2	0.1
Node 2	0.8	0.1
Node 3	2	0.1

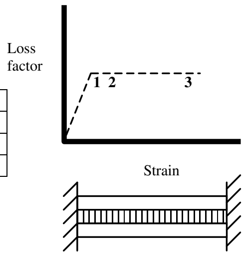

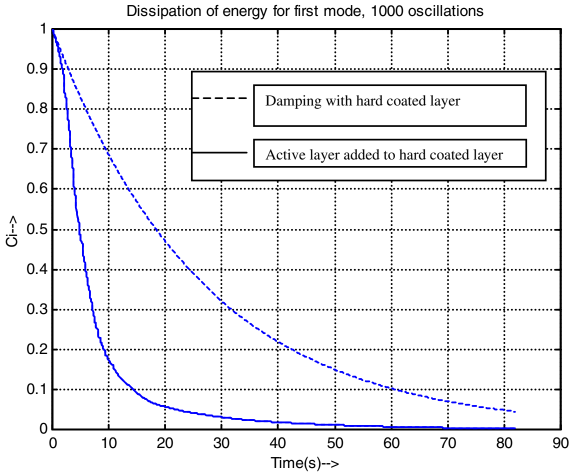

Figure 11. Damping of vibration using a sandwiched strain-dependent damping layer and using the same in combination with an active layer.

4. Hard-coated damping layer is Oberst:

	Strain (X10^{-4})	Loss factor
Node 1	0.2	0.1
Node 2	0.8	0.1
Node 3	2	0.1

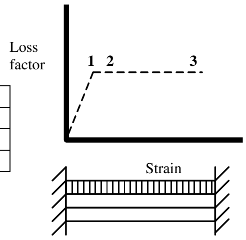

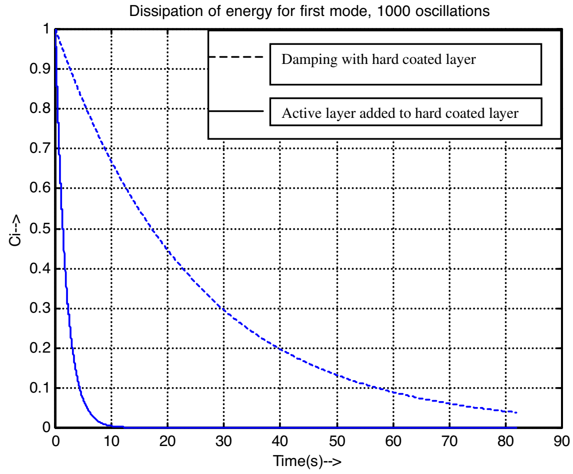

Figure 12. Damping of vibration using an Oberst strain-dependent damping layer and using the same in combination with an active layer.

Acknowledgment

The authors would like to acknowledge the Aeronautical Research and Development Board (India) for partially supporting the research work.

References

[1] Anderson E H, Lindler J E and Regelbrugge M E 2002 Smart material actuator with long stroke and high power output *43rd AIAA/ASME/ASCE/AHS/ASC Structures, Structural Dynamics and Materials Conf.* AIAA 2002-1354

[2] Baz A and Ro J 1994 The concept and performance of active constrained layer damping *J. Sound Vib.* **28** 18–21

[3] Baz A and Ro J 1996 Vibration control of plates with active constrained layer damping *Smart Mater. Struct.* **5** 272–80

[4] Shen I Y 1994 Hybrid damping through active constrained layer treatments *ASME J. Vib. Acoust.* **116** 341–9

[5] Tani T, Tagaki T and Qiu J 1998 Intelligent material systems: application of functional materials *Appl. Mech. Rev.* **51** 502–21

[6] Sandlund L, Fahlander M, Cedell T, Restorff J and Clark A E 1994 Magnetostriction, elastic moduli and coupling factors of composite Terfenol-D *J. Appl. Phys.* **75** 5656–8

[7] Liao W H and Wang K W 1996 A new active constrained layer configuration with enhanced boundary actions *Smart Mater. Struct.* **5** 638–48

[8] Lim Y H, Varadan V V and Varadan V K 2002 Closed loop finite element modelling of active constrained layer damping in the time domain analysis *Smart Mater. Struct.* **11** 89–97

[9] Bhattacharya B, Rongong J A and Tomlinson G R 1999 Vibration suppression performance of piezoceramic and magnetostrictive materials in hybrid constrained layer damping *SPIE 6th Ann. Int. Conf. on Smart Structures and Materials (Newport Beach, CA, March 1999)* (Paper 3672-27)

[10] Giauque Karimmi P H, Sagradi M, Barbezat G and Salito A 1998 High damping capacity iron–chromium–aluminium based coatings for surface vibration control *Proc. 15th Int. Thermal Spray Conf. (Nice, May 1998)* pp 581–6

[11] Bhattacharya B, Vidyashankar B R, Patsias S and Tomlinson G R 2000 Active and passive vibration control of flexible structures using a combination of magnetostrictive and ferro-magnetic alloys *SPIE Int. Symp. on Applied Photonics (Glasgow, May 2000)*

[12] Patsias S, Saxton C and Shipton M 2004 Hard damping coatings: an experimental procedure for extraction of damping characteristics and modulus of elasticity *Mater. Sci Eng.* A **370** 412–6

[13] Lim S R, Kim S Y, Kang J K, Park J T and Son D 1999 Magnetostrictive properties of polymer-bonded Terfenol-D composites *J. Magn. Magn. Mater.* **191** 113–21

[14] Van Nostrand W C, Knowles G J and Inman D J 1993 Active constrained layer damping for micro-satellites *Dynamics and Control of Structures in Space, Proc. 2nd Int. Conf. (Cranfield, UK, 6–10 Sept)* A95-91373, pp 667–81

[15] Thomson W T 1999 *Theory of Vibration with Applications* 4th edn (Englewood Cliffs, NJ: Prentice-Hall)

[16] Sagradi D P, Sagradi M and Martin J L 2001 Noise and vibration damping of Fe–Cr–X alloys *J. Braz. Soc. Mech. Sci.* **23** 115–22